Effect of Surface Cooling and Roughness on Transition for the Shuttle Orbiter

John J. Bertin* and E. S. Idar III†
The University of Texas at Austin, Austin, Texas
and
Winston D. Goodrich‡
NASA Johnson Space Center, Houston, Texas

An analysis of roughness-induced boundary-layer transition examines the sensitivity of the Orbiter boundary-layer transition criteria to surface cooling, surface roughness, and the assumed flowfield model. The experimental data were obtained in tunnel B (AEDC) using a 0.0175-scale Orbiter with surface roughness elements simulating misaligned heatshield tiles for surface temperatures from 0.12 T_t (a value typical of entry conditions) to 0.42 T_t (a value typical of continuous-flow wind tunnels). Tile misalignment had only a slight effect on the heat transfer and transition locations for $T_w = 0.42\ T_t$. Cooling the boundary layer caused the tile-induced disturbances to increase significantly, promoting premature transition. Correlation of the effects of the misalignment height and of surface cooling in promoting transition are presented, and predictions made for typical Orbiter entry conditions.

Nomenclature

h = local heat-transfer coefficient, $\dot{q}/(T_t - T_w)$
$h_{t,\mathrm{ref}}$ = heat-transfer coefficient for the stagnation point of the reference sphere
k = height of the misaligned tiles
k_a = allowable tile misalignment height for relative transition locations calculated using Eq. (3)
L = axial model length, 0.5734 m (1.881 ft)
M_∞ = freestream Mach number
$\dot{q}$ = local heat transfer rate
r_{ref} = radius of the reference sphere, 0.00533 m (0.0175 ft)
Re_{ns} = Reynolds number based on flow conditions just downstream of a normal shock and the reference radius
$Re_{\infty,L}$ = Reynolds number based on freeestream flow poperties and the model length
T_t = stagnation temperature
T_w = wall temperature
x = axial coordinate
x_{tr} = axial coordinate at the transition location
δ^* = displacement thickness
ξ = correlation for all the experimentally determined relative transition locations, Eq. (3)
ξ_1 = relative transition location defined in Eq. (1)
ξ_2 = relative transition location defined in Eq. (2)

Introduction

THE design of the windward heatshield of the Shuttle Orbiter depends strongly on the heating rates encountered during atmospheric entry. Specifically, the local magnitudes and overall distribution of heating are known to be sensitive to the character of the boundary layer, i.e., laminar, transitional, or turbulent. Consequently, factors which alter the location of boundary-layer transition should be identified and transition criteria developed to avoid an unnecessarily conservative heatshield design. However, because of the complexity of the transition process and the large number of interrelated parameters which influence the transition location, a theoretical prediction of transition is impossible. Thus, experimental programs were conducted to provide a data base for use in developing transition correlations for the Shuttle Orbiter. Because the windward surface is composed of a large number of thermal protection tiles, the transition correlations must include the effect of the distributed roughness arising from the joints and possible tile misalignment.

Heat-transfer data[1] obtained in tunnel B of the Arnold Engineering Development Center (AEDC) for an 0.04-scale Orbiter indicated that a ring of spherical trips, which were 0.079 cm (0.031 in.) in diameter and were $0.11L$ from the nose, caused the transition location to move considerably upstream of the natural transition location (i.e., that for a smooth body). In the same test program, a simulated interface gap between two insulation materials, which was 0.102 cm (0.040 in.) wide by 0.203 cm (0.080 in.) deep and was located at $x = 0.02L$, had no measurable effect on boundary-layer transition at $\alpha = 40$ deg and $Re_{\infty,L} = 8.6 \times 10^6$. In a series of tests using delta-wing Orbiter models,[2] premature boundary-layer transition was observed on a model having simulated heatshield panels with raised joints. Slot joints, however, did not cause premature transition of the boundary layer. The former model featured a series of transverse panels 0.635 cm (0.250 in.) wide, separated by a raised retaining strip 0.025 cm (0.010 in.) wide by 0.0025 cm (0.001 in.) high. The panels on the model with slotted joints were 0.635 cm (0.250 in.) square, separated by slots 0.020 cm (0.008 in.) wide by 0.005 cm (0.002 in.) deep. The Reynolds number ($Re_{\infty,L}$) for these tests ranged from 6.5×10^6 to 9.0×10^6 using a model 0.403 m (1.321 ft) long.

Data from an experimental program which was conducted to investigate what effect tile misalignment, representative of a reasonable manufacturing tolerance, has on heat transfer and transition criteria in the plane-of-symmetry of the Shuttle

Presented as Paper 77-704 at the AIAA 10th Fluid and Plasmadynamics Conference, Albuquerque, N. Mex., June 27-29, 1977; submitted July 11, 1977; revision received Nov. 15, 1977.

Index categories: Boundary-Layer Stability and Transition; Supersonic and Hypersonic Flow.

*Professor, Dept. of Aerospace Engineering and Engineering Mechanics. Associate Fellow AIAA.
†Research Assistant, Dept. of Aerospace Engineering and Engineering Mechanics; currently with General Dynamics, Ft. Worth Division.
‡Aerospace Technologist, Aerothermodynamics Section. Associate Fellow AIAA.

Orbiter, have been analyzed.[3] The vertical tile misalignment simulated on the 0.0175-scale model was approximately 0.1451 cm (0.0571 in.) full-scale. Futhermore, the surface temperature for the tunnel B tests was essentially constant at 0.42 T_t. As noted in Ref. 3, the presence of tile misalignment did not significantly affect the transition locations over the range of test conditions considered. A complementary test program was conducted in tunnel F, where the windward surface was roughened by a grit blasting technique. The surface temperature for the tunnel F tests varied from 0.14 T_t to 0.28 T_t. At the higher Reynolds numbers of the tunnel F tests, the transition location moved near the nose. At these test conditions, the roughness elements became large relative to the boundary layer and became effective as tripping elements.

Using another set of data obtained in tunnel B, Hube[4] observed that "projecting tiles were effective boundary-layer trips." The height of the transition-promoting tiles corresponded to a full-scale tile misalignment of 0.3175-1.5875 cm (0.1250-0.6250 in.).

Unless the model is heated or cooled, the surface temperature of a tunnel B model is approximately 0.42 T_t. However, a surface temperature of 0.12 T_t is more typical of entry conditions important to vehicle design. The stability of laminar boundary layers has been found to be significantly affected by heating or cooling (usually indicated parametrically by a temperature ratio, or enthalpy ratio, such as T_w/T_r). Lees[5] found that heat-transfer from the fluid to the wall stabilized a laminar boundary layer for two-dimensional disturbances. However, the unqualified prediction that cooling stabilizes the boundary layer cannot be made since, as a result of cooling the boundary layer, there is a relative increase in the magnitude of disturbance due to a fixed roughness.[6] A further complication is associated with wind tunnel data. Since a low value of T_w/T_r may be obtained either by cooling the wall or by heating the test gas, alternative effects may arise. Using data from a single tunnel, Wagner et al.[7] noted that reducing T_w/T_r by heating the flow significantly decreased $Re_{s,tr}$, possibly because of nonuniform mixing of the supply gas in the stagnation chamber.

This paper presents flowfield and data correlations which relate the location of boundary-layer transition on the Shuttle Orbiter to the simulated heat-shield tile misalignment heights and a single boundary-layer parameter (δ^*), which incorporates the effects of flowfield conditions and surface temperature. In addition, this paper presents theoretical heat-transfer distributions, which are compared with experimental heat-transfer distributions obtained in tunnel B, using a 0.0175-scale model of the Space Shuttle Orbiter configuration, for which the first 80% of the windward surface was roughened by a simulated tile misalignment. The experimental heat-transfer data were used to determine the transition locations. Data were obtained for a Mach number of 8 over a Reynolds number range (based on model length) from 1.862×10^6 to 7.091×10^6, with surface temperatures from 0.114 T_t to 0.435 T_t.

Experimental Program

The primary objective of the present investigation was to determine what effect tile misalignment, representative of a reasonable manufacturing tolerance, has on the heat-transfer distribution in the plane of symmetry of the Shuttle Orbiter over a wide range of surface temperature. To do this, the heat-transfer data from three test programs conducted in tunnel B were studied. The data were obtained at a freestream Mach number of 8 over a range of freestream Reynolds number (based on model length) from 1.862×10^6 to 7.091×10^6. The surface temperature was varied from 0.114 T_t to 0.435 T_t. The data presented in this paper were obtained at angles-of-attack of 30 and 40 deg. For additional information about the test conditions, the model, and the data, the reader is referred to Refs. 8-12.

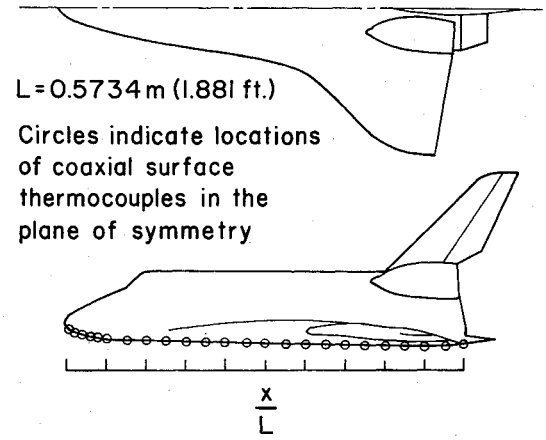

Fig. 1 Sketch of Space Shuttle Orbiter model.

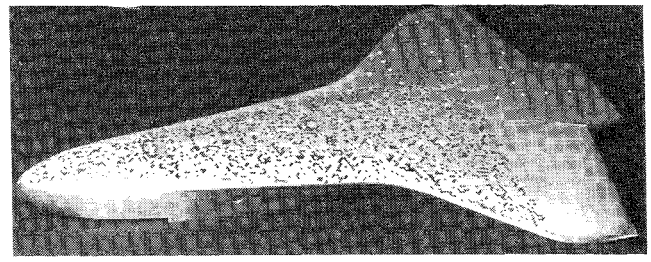

Fig. 2 Photograph of model showing randomly misaligned tiles.

Models

The basic model used in the test programs (Fig. 1) was a 0.0175-scale model of the Space Shuttle Orbiter configuration defined by Rockwell drawing VL70-000139 and designated Model 29-0. Coaxial surface thermocouples were used to obtain the heat-transfer rate distributions for the windward plane-of-symmetry. The locations of the heat-transfer gages in the windward plane-of-symmetry are indicated in Fig. 1. To study the effect of tile misalignment, selected tiles were precisely etched (or deposited, as discussed in Ref. 9, depending on the misalignment height) on the windward surface, so that they were slightly above the model surface. The misaligned tiles formed a herringbone pattern (symmetric about the plane of symmetry) covering the windward surface of the Orbiter model up to the tangent line of the chines from $x = 0.02L$ to $0.80L$. The raised tiles, selected randomly, represented 25% of the tiles in the area of interest, as shown in Fig. 2. The selected tiles were 0.267 cm (0.105 in.) square. The model surface for each of the three test programs is summarized below.

Smooth Body Test Program

For these tests, the surface of the 0.0175-scale Orbiter model was smooth. Thus, the transition locations, determined from the heat-transfer distributions for the smooth body (designated k_o), serve as the reference transition locations. The reader is referred to Ref. 10 for the basic data and for additional information regarding these tests.

Vertically Misaligned Tiles (k_1) Test Program

For these tests, the misaligned tiles were deposited to a height of approximately 0.0025 cm (0.0010 in.). The vertical misalignment, thus simulated, was 0.1451 cm (0.0571 in.) full-scale. The basic data for this tile misalignment height (designated k_1) are presented in Ref. 11. A brief analysis of the heat-transfer data and the transition locations was presented in Ref. 3.

Vertically Misaligned Tiles (k_2) Test Program

For these tests, the surface surrounding the tiles was removed until the misaligned tiles were approximately 0.0051

cm (0.0020 in.) in height. This misalignment (designated k_2) corresponds to a full-scale vertical misalignment of 0.2903 cm (0.1143 in.). Additional information about the model and basic data for this test program are presented in Ref. 12.

Discussion of Results

The effects of the height of the misaligned tiles and the surface temperature on the heat-transfer distribution for the plane of symmetry when the Orbiter is at an angle of attack of 30 deg are illustrated in the data presented in Fig. 3. Data are presented from tests where the freestream Mach number was 8.0, the freestream Reynolds number based on the model length was 7.0×10^6, and the surface temperature was either 300 K (0.40 T_t) or in the range of 96-127K (0.128T_t-0.171T_t). The heat-transfer distributions are presented as the dimensionless ratio, $h/h_{t,\,ref}$, which involves the experimental value of the local heat-transfer rate divided by theoretical value of the heat-transfer rate to the stagnation point of a 0.00533 m (0.0175 ft) radius sphere, as calculated using the theory of Fay and Riddell.[13] For purposes of data presentation, the recovery factor has been set equal to unity.

Heat-transfer distributions for theoretical solutions of a nonsimilar laminar boundary layer using the small crossflow axisymmetric analog to represent the three-dimensional character of the boundary layer, which were calculated using the numerical code of Ref. 14, are included in Fig. 3. Required as input for the boundary layer code were the static pressures, the entropy at the edge of the boundary layer, and the radius of the "equivalent" body of revolution. Because the bow shock wave is curved, the entropy varies throughout the shock layer. Thus, for the flow model which is designated as the "variable entropy" flow model, the local flow properties at the edge of the boundary layer were evaluated using the entropy and the surface pressure distributions calculated using the numerical code of Ref. 15. The variation of the local entropy at the edge of the boundary layer, due to variation in the local boundary layer thickness (which is Reynolds number dependent), was believed to be of second-order importance for the present application and was, therefore, neglected. The heating distributions calculated using this variable entropy flow model are in good agreement with the laminar data, especially for $x \geq 0.2L$. Theoretical values for the nondimensionalized heat-transfer coefficient were slightly greater for the colder surface, i.e., $T_w = 0.131\ T_t$. The increased heating is attributed to the increased velocity gradients and viscous dissipation, which result when the boundary-layer thickness is decreased by surface cooling, i.e., as T_w/T_t decreases. The data presented in Fig. 3 are consistent with the theoretically determined effect of surface temperature. Study of additional data from these tests indicates[8] that there was no clear correlation between the experimental values of the nondimensionalized local heating and the surface temperature. This lack of correlation is of little significance, since the theoretical solutions predict less than a 15% change in heat-transfer level, and the experiment was not designed to resolve changes of this magnitude.

The heat-transfer distributions were used to determine the "point" at which boundary-layer transition location occurred in the plane of symmetry. The experimentally determined transition location was that point at which the heat transfer deviated from the laminar distribution. The transition locations from selected tests are presented in Fig. 3. At the higher surface temperature, the misaligned tiles moved transition only slightly upstream relative to the smooth-body transition location (refer to the open symbols in Fig. 3). However, at the lower temperature and for greater tile misalignment, tiles which were misaligned 0.0025 cm (k_1) moved transition forward by 0.1L, and increasing the tile misalignment height to 0.0051 cm (k_2) moved transition well forward. For lower surface temperature and for greater tile misalignment, transition occurred very near the nose, approaching a minimum transition length. The tile-induced

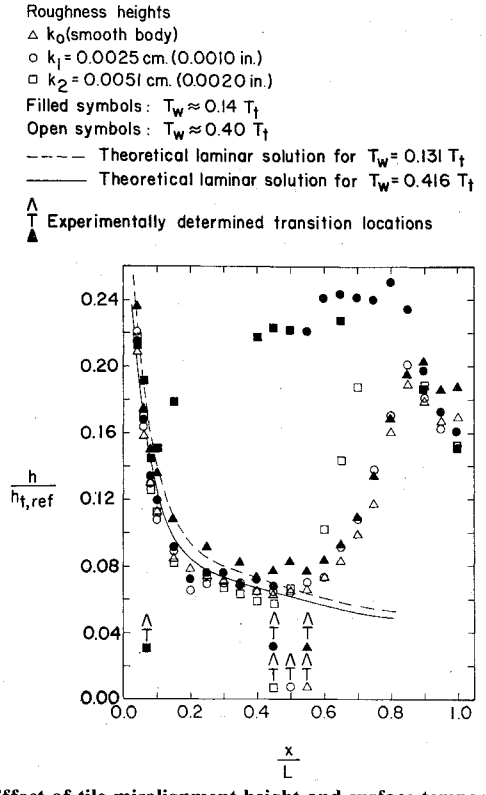

Fig. 3 Effect of tile-misalignment height and surface temperature on heat-transfer distribution, $\alpha = 30$ deg, $Re_{\infty,L} = 7.0 \times 10^6$.

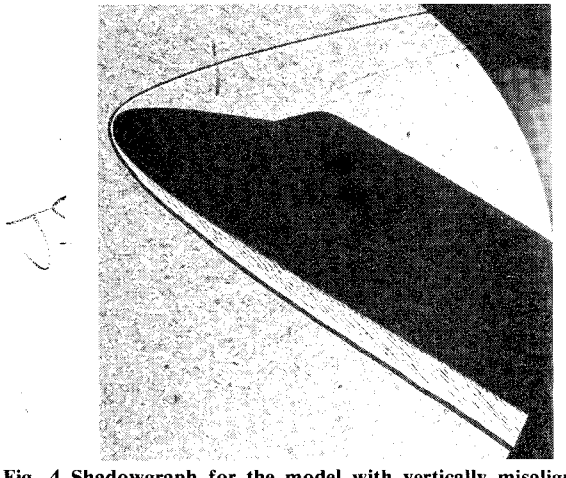

Fig. 4 Shadowgraph for the model with vertically misaligned tiles (i.e., $k_2 = 0.0051$ cm) at $\alpha = 30$ deg, $Re_{\infty,L} = 7.0 \times 10^6$, $T_w = 0.171T_t$.

boundary-layer perturbation appears to be a function of the height of the tile relative to the displacement thickness. A correlation of the transition location in terms of the displacement thickness includes the interdependence between the local Mach number, Reynolds number, surface temperature, and tile misalignment height.

Theoretical Mach number profiles indicated[8] that the misaligned tiles would protrude into the sonic regions of an unperturbed laminar boundary layer over much of the body. Thus, one would expect that the presence of the misaligned tiles would significantly perturb the flowfield. This is verified in the shadowgraph of Fig. 4. Easily visible waves emanate from the tiles. A highly vortical flow results when the turbulent boundary layer bounces over the misaligned tiles. Nevertheless, as can be seen in the data of Fig. 3, tile misalignment did not significantly affect the heat-transfer rates, where the boundary layer was either laminar or turbulent for the conditions of these wind tunnel tests.

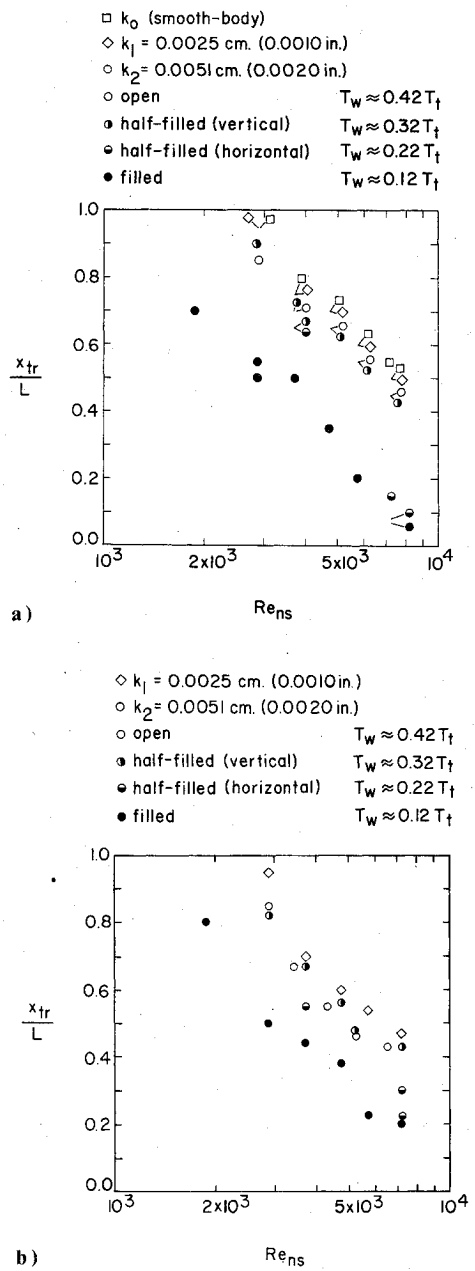

Fig. 5 Transition locations as a function of the Reynolds number behind a normal shock wave: a) $\alpha = 30$ deg, b) $\alpha = 40$ deg.

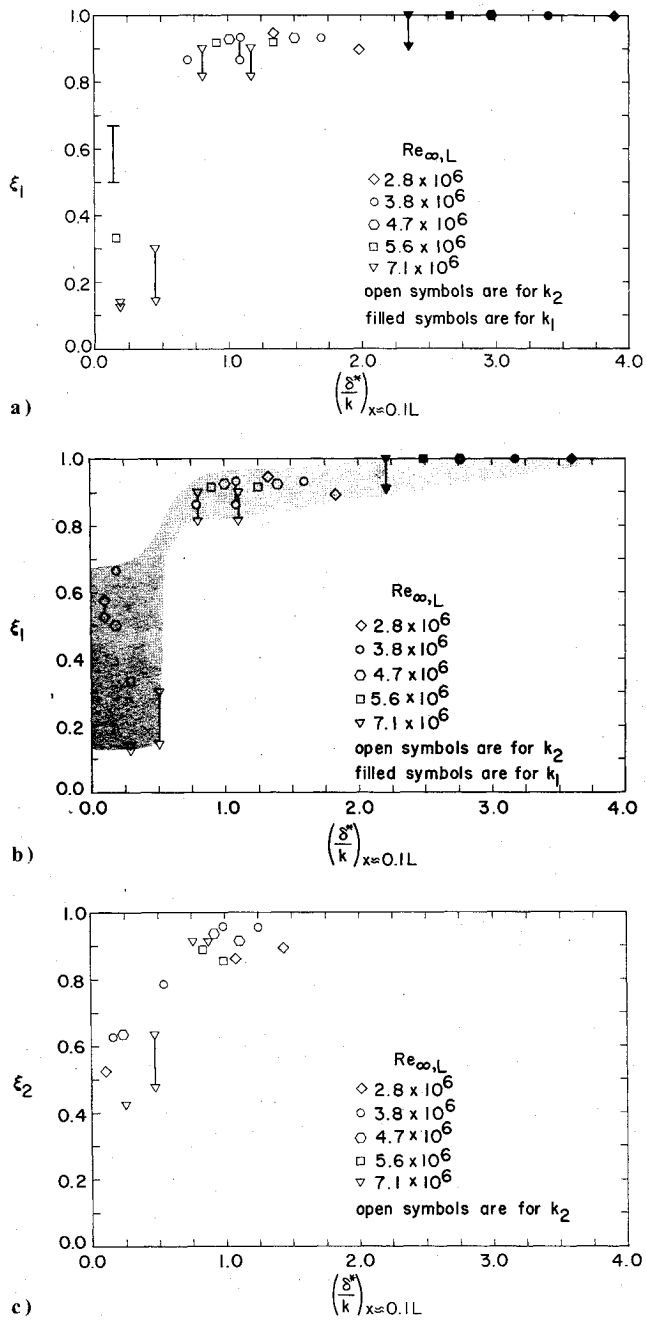

Fig. 6. The experimentally determined relative transition locations (ξ_1 or ξ_2) as a function of $(\delta^*/k)_{x=0.1L}$: a) modified Newtonian theory with normal shock entropy, $\alpha = 30$ deg, b) variable entropy theory, $\alpha = 30$ deg; c) variable entropy theory, $\alpha = 40$ deg.

The transition locations for the three test programs are presented in Fig. 5 as a function of Re_{ns}, the Reynolds number based on conditions downstream of normal shock wave and the reference radius, 0.00533 m. Although the use of a local Reynolds number would be more desirable, Re_{ns} was chosen because it was simple to calculate and yet account for variations in freestream Mach number. The transition location was a function of the angle of attack, freestream conditions (specifically, the Reynolds number, since the Mach number was essentially constant for these tunnel B tests), surface temperature, and tile misalignment height. The transition locations for a tile-roughened model, where $k = 0.0025$ cm (k_1), were essentially the same as those recorded for a smooth model. However, when the heights of the misaligned tiles were 0.0051 cm (k_2) and $T_w \approx 0.42 T_t$, the transition locations moved forward approximately $0.05L$, which is the distance between adjacent heat-transfer gages. Data were obtained for the k_2 surface finish, i.e., $k = 0.0051$ cm over a range of surface temperatures from 0.11 T_t to 0.42 T_t. Cooling the wall to 0.32 T_t did not significantly affect the transition locations. However, when the wall was cooled to 0.22 T_t or to 0.12 T_t, a dramatic forward movement of the transition location was observed. Furthermore, the relative forward movement was very sensitive to the Reynolds number.

The experimentally determined transition locations indicate that the tile-induced flow perturbations become strongest when the height of the misaligned tiles is of the order of the displacement thickness. The transition location moved significantly forward as surface cooling at the higher Reynolds numbers thinned the boundary layer. The transition location for a given perturbed flow has been divided by the corresponding location on the reference configuration. This ratio, termed the "relative transition location," is presented as a function of δ^*/k in Fig. 6. In these correlations, δ^*/k is evaluated at $x \approx 0.1L$. This axial location was chosen because it is near the forward-most transition location (and, therefore,

approximately represents the limiting effect of a boundary-layer tripping element), but is not in the stagnation region (over this range of α) where it would be difficult to calculate the displacement thickness of the highly cooled, accelerating boundary layer. Since smooth-body data[10] were obtained only for angles of attack of 25, 30, and 35 deg, the reference transition locations for an α of 40 deg were those for the k_1 tile-roughened model.[11] This approximation was made since there was no consistently measurable difference between the transition location for the smooth body (k_o), and those for the k_1 tile-roughened model ($k = 0.0025$ cm) for an α of 30 deg (see Fig. 5). Thus, the relative transition locations for $\alpha = 30$ deg are presented as the ratio ξ_1, where

$$\xi_1 = \frac{(x_{tr}/L)_{k_i, T_{wi}, Re_{ns}}}{(x_{tr}/L)_{k_O, 0.42T_t, Re_{ns}}} \tag{1}$$

For $\alpha = 40$ deg, the relative transition locations are presented as the ratio ξ_2, where

$$\xi_2 = \frac{(x_{tr}/L)_{k_i, T_{wi}, Re_{ns}}}{(x_{tr}/L)_{k_1, 0.42T_t, Re_{ns}}} \tag{2}$$

These nondimensionalized, relative transition-locations represent the ratio of the experimentally determined transition location at the tile misalignment height of a particular run (k_i), at the surface temperature of that run (T_{wi}), and at the Reynolds number of that run, divided by the transition location measured at the same Reynolds number but at the reference surface finish (either k_o or k_{11}), and at the reference surface temperature (0.42 T_t).

The values of δ^*/k at $x \approx 0.1\,L$ were calculated for a nonsimilar laminar boundary layer. For some conditions, boundary-layer transition occurred slightly upstream of these x locations. Thus, the actual value of δ^* for these cases would be significantly different than the calculated value. Theoretical solutions were generated with a "modified Newtonian with normal shock entropy" flow model at $\alpha = 30$ deg, for the "variable entropy" flow model at $\alpha = 30$ deg, and for the variable entropy flow model at $\alpha = 40$ deg. The correlations obtained, using the modified Newtonian with normal shock entropy flow model, are included to illustrate what effect the assumed flow model has on the correlations. For the relatively simple modified Newtonian with normal shock entropy flow model, the fluid at the edge of the boundary layer was assumed to be that which had passed through the normal portion of the bow shock wave, and had accelerated isentropically from the stagnation point to the local static pressure, which was calculated using modified Newtonian theory. Neither of the theoretical flow models reflect tile-induced peturbations.

The relative transition location ξ is near unity (i.e., the tile-induced perturbations have negligible effect on the transition location) at the higher values of δ^*/k. As δ^*/k is decreased, i.e., the boundary layer is cooled, the Reynolds number is increased, or the tile misalignment height is increased, transition moves gradually forward, that is, ξ decreases slowly. In this region, where $0.9 < \xi < 1.0$, the magnitude of ξ does not exhibit any dependence on the Reynolds number, except through the value of δ^*/k. Below a critical value of the δ^*/k, the relative transition location decreases rapidly (i.e., transition moves rapidly upstream toward the nose) as the boundary layer thins. Below the critical value of δ^*/k, the Reynolds number has a strong effect on the magnitude of ξ. Note that the critical value of δ^*/k, evaluated at $x \approx 0.1L$, is independent of the flowfield model used in the calculation of δ^* and the local Reynolds number, and is independent of the angle of attack for *these wind tunnel results*.

The relative transition locations for both angles of attack are presented in Fig. 7 as a function of the theoretical laminar values of δ^*/k at $x \approx 0.1\,L$ for both flow models. Note that,

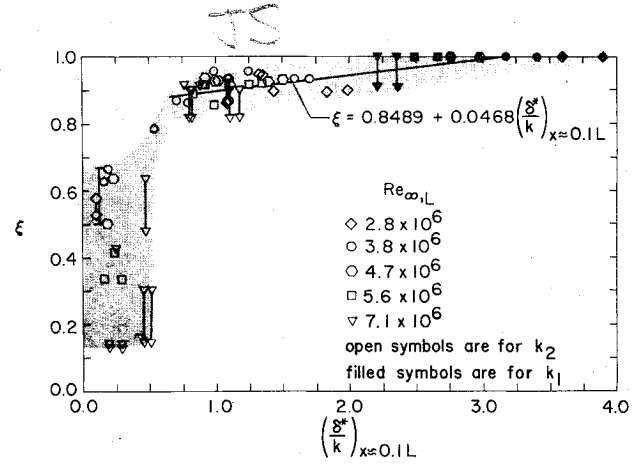

Fig. 7 Relative transition locations for both angles of attack as a function of the theoretical laminar values of $(\delta^*/k)_{x \approx 0.1L}$ for both flow models.

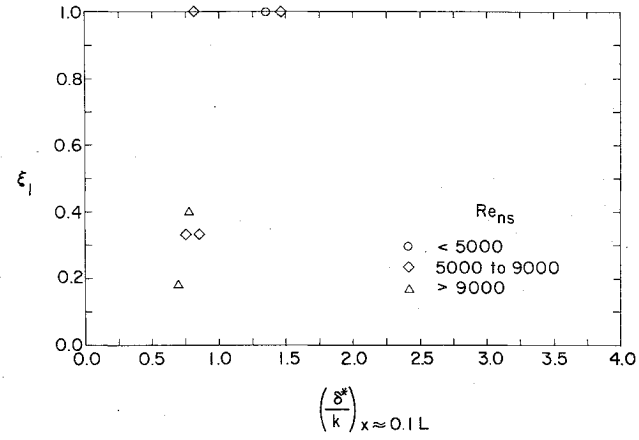

Fig. 8 Relative transition locations ξ_1 for a grit-roughened model tested in tunnel F as a function of $(\delta^*/k)_{x \approx 0.1L}$, $\alpha = 30$ deg.

for $\delta^* \geq 0.75k$, the experimental values of $\xi \geq 0.81$, i.e., the roughness-perturbed transition locations, are within 19% of the reference smooth-body transition locations. At the lowest surface temperatures, δ^* was so thin, i.e., $\delta^* < 0.75k$, that the presence of the misaligned tiles moved transition well upstream. Using a linear least-squares fit of those data, for which δ^* at $x \approx 0.1L$ was greater than $0.75k$, yields the correlation

$$\xi = 0.8498 + 0.0468\,(\delta^*/k)_{x \approx 0.1L} \tag{3}$$

which is valid for both angles of attack and for both flow models. Using this correlation, when $\delta^* = 0.75k$, $\xi = 0.884$. Thus, the "nominal" transition location moves upstream by just over 10% when $\delta^* \sim K$.

When a correlation to predict the transition location for a particular configuration is developed, using data from a single-wind tunnel, one must ask how general such a correlation is. Differences in the transition locations obtained in different tunnels may be due to tunnel noise, nonuniform mixing of the relatively high-temperature flows, or other related tunnel factors. Thus, the parameters used to correlate the tunnel B data in Fig. 6, were also used to correlate data obtained on a similar model in tunnel F. For the tunnel F tests (Refs. 16 and 17), the Mach number varied from 10.73 to 12.06 while the freestream Reynolds number (based on model length) varies from 1.17×10^6 to 17.63×10^6. The surface temperature varied from $0.16T_t$ to $0.27\,T_t$. The surface was roughened over the first 80% of the windward surface using a grit-blasting technique. The average peak-to-valley distance for ten readings in a 0.25 cm (0.10 in.) length, as read from a

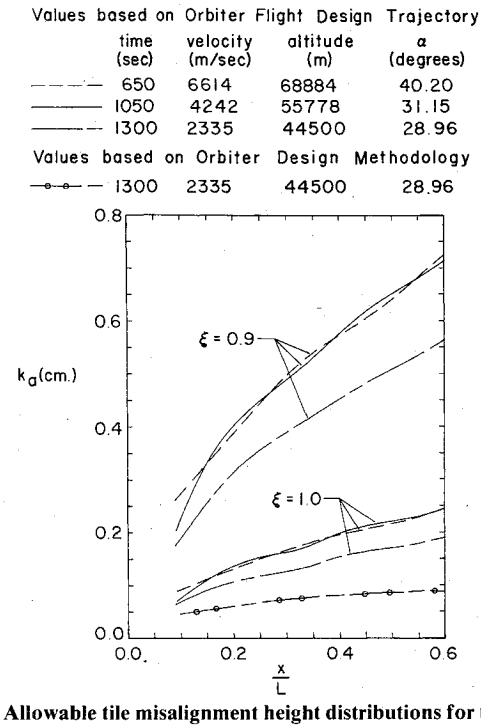

Fig. 9 Allowable tile misalignment height distributions for the Orbiter at flight conditions.

photomicrograph, was 0.0041 cm (0.0016 in.). The fact that the transition locations for the roughened models were obtained at slightly different flow conditions than those for the smooth models introduces uncertainties in the values of ξ_1 for these tunnel F tests. Nevertheless, as illustrated by the data presented in Fig. 8, only when δ^* at $x \approx 0.1L$ (as calculated using the variable entropy flow model) was less than $0.85k$, did the presence of surface roughness move transition well upstream. It is significant that the critical value of δ^*/k is essentially the same for the data from the two tunnels. The agreement is especially significant, since, for the tunnel B tests, the surface was roughened by misaligned tiles but, for the tunnel F tests, it was roughened by a grit-blasting technique.

Figure 9 illustrates the application of the correlation defined by Eq. (3) to establish allowable tile misalignment height distributions for the Orbiter at flight conditions. Predictions of the Orbiter three-dimensional flowfield and boundary-layer parameters, made using the methods of Ref. 15, were used to define δ^* along the Orbiter windward surface for selected times during the design trajectory. The simpler, but less realistic, modified Newtonian with normal shock entropy flowfield predicted values of δ^*, which were roughly 50% larger than the variable entropy flowfield methods described in Ref. 15. Therefore, the modified Newtonian with normal shock entropy flow methods should not be used in extrapolating the k_a correlation to flight conditions if high accuracy is desired, even though the differences between the two flow model correlations are small at wind tunnel conditions.

Allowable values of k_a are defined as misalignment heights, which, for given flow conditions, do not alter the smooth-body boundary-layer transition location significantly, i.e., having values of ξ near one. Specifically, allowable roughness heights along the Orbiter centerline, which do not cause transition to move from the natural (or smooth-body) locations for a given flow condition, can be defined by restricting ξ to a value of 1.0 and solving Eq. (3) for k_a when the distribution of δ^* is known. Similarly, a relaxed criteria for k_a may be defined by allowing transition to move 10% forward of the natural transition location. These values of allowable tile misalignment height distribution can be calculated by repeating the aforesaid procedure with $\xi = 0.9$. Distributions of k_a along the Orbiter centerline are presented in Fig. 9 for $\xi = 1.0$ and 0.9 for three flow conditions taken from the entry design trajectory. These flow conditions, which represent a wide range of hypersonic flows, cover the major part of the Orbiter entry trajectory where significant aerodynamic heating occurs. This range includes the high hypersonic phase, when natural transition begins to occur on the aft end of the centerline ($t = 1050$ s), and the low hypersonic phase, when natural transition has moved up to approximately $x = 0.2L$ ($t = 1300$ s).

Figure 9 illustrates several points concerning allowable roughness, or heatshield tile misalignment, for the Orbiter. First, the minimum values of k_a are established by later trajectory conditions for stations where natural transition has not occurred (e.g., for $x \leq 0.2L$ when $t \approx 1300$ s), since these flow conditions produce the highest local Reynolds number and the thinnest boundary layers. Second, allowable roughness heights vary significantly with location and increase as x/L increases. This is consistent with the fact that both the boundary-layer thickness and related parameters increase with distance. Perhaps the most significant point illustrated in Fig. 9 is that k_a can be increased by a factor of 3 if the location of boundary-layer transition is allowed to move 10% forward of natural transition (i.e., calculating k_a using $\xi = 0.9$ instead of 1.0). Finally, predictions based on the correlation developed herein indicate that the current design methodology used to predict k_a for the Orbiter appears to be conservative, even when compared to the present correlation with $\xi = 1.0$. Figure 9 suggests that k_a can be easily increased to 3 times the value, based on the current design methodology, and still not move boundary-layer transition forward more than 10%.

The temptation to relax the current Orbiter design methodology for k_a should be tempered by the fact that the scope of the heatshield roughness problem is actually much broader than roughness-induced boundary-layer transition. For example, local heating roughness elements (e.g., heatshield tile corners, etc.) must be assessed for both laminar and turbulent flows before electing to increase k_a to the values indicated in Fig. 9. However, a significant part of this design problem appears to have been clarified as a result of this investigation. That is, the boundary layer transition for the Orbiter is not nearly as sensitive to surface roughness caused by misaligned heatshield tiles as previously believed.

Concluding Remarks

Theoretical flowfield parameters and heat-transfer distributions were used to analyze and correlate experimental heat-transfer and boundary-layer transition data using a 0.0175-scale model of the Space Shuttle Orbiter, for which the first 80% of the windward surface was roughened to simulate misaligned tiles. Data were obtained for a Mach number of 8 over a Reynolds number range (based on model length) from 1.862×10^6 to 7.091×10^6, with surface temperatures from 0.114 T_t to 0.435 T_t. For the geometries and for the flow conditions of the present wind tunnel test programs, the following conclusions are made.

1) Theoretical solutions indicate that thinning the boundary layer by surface cooling increased the nondimensionalized value of the local heat-transfer coefficient. The theoretical increase was due to the increased gradients and viscous dissipation which result when the boundary-layer thickness decreased. However, the coaxial surface thermocouples used to measure the heating rates were not sufficiently accurate to show the variations of the magnitude predicted by theory.

2) Tile misalignment did not significantly affect the heat-transfer rates in regions where the boundary layer was either laminar or turbulent. This does not exclude the possibility of locally high heating to very small regions (such as tile corners) which could not be measured.

3) When δ^* at $x \approx 0.1L$ was equal to or greater than $0.75k$, the experimentally determined transition locations for a tile-roughened cooled model were within 19% of the reference smooth-body transition location at the same freestream conditions. The tile-induced flow perturbations caused significant forward movement of transition only when the theoretical value of δ^* at $x \approx 0.1L$ was less than $0.75k$.

4) The critical value of δ^*/k at $x \approx 0.1L$ was independent, both of the flowfield model used to calculate δ^* and of the angle of attack for *these wind tunnel tests*. However, the accurate prediction of k_a requires that the variation of entropy along the edge of the boundary layer be taken into account in the calculation of δ^*.

References

[1] Carver, D. G., "Heat-Transfer Tests on the Rockwell International Space Shuttle Orbiter with Boundary-Layer Trips (OH-54)," AEDC-TR-76-28, May 1976.

[2] Seegmiller, H. L., "Effects of Roughness on Heating and Boundary Layer Transition, Part I - Effects of Simulated Panel Joints on Boundary-Layer Transition," *Space Shuttle Aerothermodynamics Technology Conference, Vol. II - Heating*, NASA TMX-2507, Feb. 1972.

[3] Bertin, J. J., Stalmach, D. D., Idar E. S. III, Conley, D. B., and Goodrich, W. D., "Hypersonic Heat-Transfer and Transition Correlations for a Roughened Shuttle Orbiter," presented at the 13th Annual Meeting of the Society of the Engineering Sciences, Hampton, Va., Nov. 1976, NASA CP-2001.

[4] Hube, H. K., "Simulated Thermal Protection Tile Roughness Effects on Windward Surface Heat Transfer on the Rockwell International Space Shuttle Orbiter," AEDC-TR-76-98, Jan. 1977.

[5] Lees, L., "The Stability of the Laminar Boundary Layer in a Compressible Fluid," NACA Rept. No. 876, 1947.

[6] Potter, J. L. and Whitfield, J. D., "The Relation Between Temperature and the Effect of Roughness on Boundary-Layer Transition," *Journal of the Aerospace Sciences*, Vol. 28, Aug. 1961, pp. 663-664.

[7] Wagner, R. D., Maddalon, D. V., Weinstein, L. M., and Henderson A. Jr., "Influence of Measured Free-Stream Disturbances on Hypersonic Boundary-Layer Transition," AIAA Paper 69-704, presented at 2nd Fluid and Plasma Dynamics Conference, San Francisco, June 1969.

[8] Bertin, J. J., Idar, E. S. III, and Galanski, S. R., "The Effect of Surface Cooling and of Roughness on the Heat-Transfer Distributions and on the Transition Locations for the Shuttle Orbiter," The University of Texas at Austin, Aerospace Engineering Rept. 77002, April 1977.

[9] Stalmach, C. J. Jr. and Goodrich, W. D., "Aeroheating Model Advancements Featuring Electroless Metallic Plating," *Proceedings of the AIAA 9th Aerodynamic Testing Conference,* Arlington, Texas, June 1976.

[10] Martindale, W. R. and Trimmer, L. L., "Test Results from the NASA/Rockwell International Space Shuttle Test (OH4A) Conducted in the AEDC-VKF Tunnel B, " AEDC-DR-74-39, May 1974.

[11] Silver, L. G. and Martindale, W. R., "Test Results from the NASA Space Shuttle Orbiter Heating Test (MH-2) Conducted in the AEDC-VKF Tunnel B," AEDC-DR-75-103, Oct. 1975.

[12] Wannenwetsch, W. D. and Martindale, W. R., "Roughness and Wall Temperature Effects on Boundary-Layer Transition on a 0.0175 Scale Space Shuttle Orbiter Model Tested at Mach Number 8," AEDC-TR-77-19, April 1977.

[13] Fay, J. A. and Riddell, F. R., "Theory of Stagnation Point Heat Transfer in Dissociated Air," *Journal of the Aeronautical Sciences*, Vol 25, Feb. 1958, pp. 73-85 and 121.

[14] Bertin, J. J. and Byrd, O. E. Jr., "The Analysis of a Nonsimilar Boundary-Layer - A Computer Code (NONSIMBL)," University of Texas at Austin, Aerospace Engineering Rept. 70002, Aug. 1970.

[15] Goodrich, W. D., Li, C. P., Houston, C. K., Chiu, P, and Olmedo, L., "Numerical Computations of Orbiter Flow Fields and Laminar Heating Rates," *Journal of Spacecraft and Rockets*, Vol. 14, May 1977, pp. 257-264.

[16] Boudreau, A. H., "Test Results from the NASA/RI Shuttle Heating Test OH-11 in the AEDC-VKF Tunnel F," AEDC-DR-74-16, Feb. 1974.

[17] Siler, L. G., "Test Results from the NASA Space Shuttle Orbiter Heating Test (MH-1) Conducted in the AEDC-VKF Tunnel F," AEDC-DR-76-13, March 1976.